isvr Institute of Sound and Vibration Research

Application of the Nonlinear Acoustic Scatter Cross-Section to the Use of Clinical Ultrasound Contrast Agents

T.G. Leighton, J.W.L. Clarke, G.J. Heald, H.A. Dumbrell and R.C. Evans

ISVR Technical Memorandum 835

Februarv 1999

University of Southampton

SCIENTIFIC PUBLICATIONS BY THE ISVR

Technical Reports are published to promote timely dissemination of research results by ISVR personnel. This medium permits more detailed presentation than is usually acceptable for scientific journals. Responsibility for both the content and any opinions expressed rests entirely with the author(s).

Technical Memoranda are produced to enable the early or preliminary release of information by ISVR personnel where such release is deemed to the appropriate. Information contained in these memoranda may be incomplete, or form part of a continuing programme; this should be borne in mind when using or quoting from these documents.

Contract Reports are produced to record the results of scientific work carried out for sponsors, under contract. The ISVR treats these reports as confidential to sponsors and does not make them available for general circulation. Individual sponsors may, however, authorize subsequent release of the material.

UNIVERSITY OF SOUTHAMPTON

INSTITUTE OF SOUND AND VIBRATION RESEARCH

FLUID DYNAMICS AND ACOUSTICS GROUP

Application of the Nonlinear Acoustic Scatter Cross-Section to the Use of Clinical Ultrasound Contrast Agents

by

T G Leighton, J W L Clarke, G J Heald, H A Dumbrell, R C Evans

ISVR Technical Memorandum No. 835

February 1999

Authorized for issue by
Professor P A Nelson
Group Chairman

ACKNOWLEDGEMENT

The authors wish to acknowledge Mr G Heald and Mr H Dumbrell of DERA Bincleaves, and Mr R C Evans of ISVR, for their contributions.

CONTENTS

FIGURE CAPTIONS

Figure 1 Illustration of the differences between the two definitions of acoustic scatter cross-section, in terms of their ability to incorporate nonlinear effects, and their ability to be interpreted in terms of the underlying bubble physics.

Figure 2 The basic definition of the second option for acoustic scatter cross-section which was introduced in figure 1.

Figure 3 The proposed modifications to be made to the acoustic scatter cross-section described in figure 2.

Figure 4 A simple scheme showing how ring-up times can be conceptualised by relating the power loss to the bubble wall velocity.

Figure 5 The effect of increasing the amplitude and duration of the driving field on the simple model introduced in figure 4.

Figure 6 Experimental arrangement for the tests undertaken in the A B Wood Laboratory.

Figure 7 Photographs of the A B Wood Laboratory (shown empty).

Figure 8 Experimental results from the A B Wood Laboratory, showing the scattered energy as the duration of the incident pulse is increased (the number of cycles in the incident pulse be appended to each curve). The peak amplitude attained by the driving pulse was constant.

Figure 9 Simulation of the effect of increasing the amplitude and duration of the incident pulse on (a) the total energy in the scattered pulse; and (b) the acoustic scatter cross-section. The peak amplitude attained by the driving pulse was 0.5 kPa (red line); 5 kPa (black line); and 10 kPa (blue line). Bubble radius: 15 micrometres; incident frequency: 200 kHz.

Figure 10 Simulation of the effect of increasing the amplitude and duration of the incident pulse on (a) the energy invested in the second harmonic in the scattered pulse; and (b) the acoustic scatter cross-section (ratio of power scattered at the second harmonic to the intensity of the incident wave). The peak amplitude attained by the driving pulse was 0.5 kPa (red line); 5 kPa (black line); and 10 kPa (blue line). Bubble radius: 15 micrometres; incident frequency: 200 kHz.

Figure 11 Conclusions from the experiments in the A B Wood tank.

Figure 12 Proposition arising form the conclusions to the experiment in the A B Wood tank.

Figure 13 Apparatus employed to measure the resonance properties of the contrast agent.

Figure 14 Simulation of the effect of increasing the amplitude and duration of the incident pulse on (a) the total energy in the scattered pulse; and (b) the acoustic scatter cross-section. The peak amplitude attained by the driving pulse was 10 kPa (red line); 30 kPa (black line); and 60 kPa (blue line). Bubble radius: 0.8 micrometres; incident frequency: 2.3 MHz.

1. INTRODUCTION

This Memorandum is based upon an Invited Address given by Dr T G Leighton to the Fourth Heart Centre European Symposium on Ultrasound Contrast Imaging (21–22 January 1999, Rotterdam, The Netherlands). Ultrasonic contrast agents are substances (most based upon gas bubbles) which are injected into the blood stream. This is done in order to enhance the ultrasonic scatter from regions of the body where the anatomy makes interpretation of the tissue-based ultrasonic information difficult (such as in the heart) [1–4]. In addition, the ultrasonic contrast agents move with the blood flow, and so are very useful in identifying flow features (including haemorrhaging) as distinct from tissue features. Not only is the direct scatter from the bubble used, but the Doppler signal is also used. Indeed the nonlinear properties of the bubble is exploited in, for example, second harmonic imaging. In this modality the second harmonic generated by the bubbles can be clearly used to identify flow features (because tissue, in comparison, produces negligible second harmonic scatter).

However, the equations used to describe or predict the behaviour of bubble dynamics are surprisingly rudimentary. Whilst nonlinear descriptions of the bubble radius motion (such as forms of Rayleigh Plesset or Herring-Keller equations) are employed in the more advanced studies, it is not uncommon to find simple linear models being used. This is particularly so when the acoustic cross-sections of the agents are considered, the fundamental physics employed being exclusively linear. This is remarkable, not only because the agents themselves are driven by sound fields of order MPa and display clear nonlinear properties (such as second harmonic scatter); but also because the acoustic methods for determining the concentration of agents are based on simply dividing the scattered energy from a bubble by an appropriate cross-section, which is exclusively derived from linear analysis. This is clearly nonsensical if significant scatter occurs in the higher harmonics. Hence the concept of the nonlinear acoustic scatter cross-section, and its use in determining the behaviour of a bubble prior to steady state (as developed under the DERA programme), has here been exploited in a study to demonstrate how the current rudimentary analysis used with contrast agents, might be extended to a more appropriate regime.

2. THEORY

Rather surprisingly, there are two descriptions of acoustic scatter cross-section which are employed in studies of contrast agents [4]. These are demonstrated in Figure 1. The first is based upon the ratio of the power scattered at the n'th harmonic, to that scattered at the fundamental, multiplied by the geometrical cross-section of the bubble. This

multiplication stage is simply an artefact to give the dimensions of area, as one would expect from a cross-section. It has no real acoustic significance otherwise, since contrast agents are rarely used in the regime where geometrical acoustics would apply. The cross-section, defined in this way, is purely empirical and based upon measurement. It does incorporate nonlinear properties, but is not related to any model of the underlying bubble physics (while such could be done, it would probably have little meaning considering the advantages of using the second definition, described next).

The second definition of the acoustic scatter cross-section is the standard one, based upon the ratio of the power scattered by the bubble, to the intensity of an incident plane wave. At current this is restricted to simple linear acoustics, but can readily be related to underlying bubble physics. That bubble physics is shown in Figure 2, where a plane wave of intensity I is incident on a bubble of radius R. Power is scattered spherically from the bubble (W_S), and can be observed at some distance r away from the bubble. The scattering cross-section, σ, is defined as the ratio W_S/I. As such it has the dimensions of power/intensity, which equal area. This basic definition can be extended to cover a bubble cloud, since if the scattering from the bubbles is incoherent, then the power detected at distance is simply summed. Hence, the cross-sections of the cloud can be determined from the number and size distribution of the bubbles, and the cross-section of those component bubbles. If multiple scattering occurs, correction factors might be employed, although there is some controversy as to what the appropriate ones might be.

The goal of the project is shown in Figure 3. The acoustic scatter cross-section, reflecting as it does the ratio of the scattered power to the incident intensity, can be interpreted in two ways. First, as described above, it represents the target area "seen" by the ultrasonic beam. Second, it might be considered to reflect the "efficiency" of the scatterer, in that the 'result' is the scattered power, and the 'input' is the incident intensity. As shown in Figure 3, the current model for the cross-section applies to steady state motion of bubbles which are behaving linearly. As such, it might be an appropriate model if the bubble is subjected to low amplitude continuous wave (*CW*) fields. However, contrast agents are almost exclusively subjected to high amplitude, short pulses (of order MPa, and of order microsecond, respectively). Therefore, the first goal of this study is to describe how the model might be modified to incorporate nonlinear, time-dependent scatter, and hence be relevant to insonation by short, high amplitude pulses. This then leads to the second goal, an investigation to determine whether it would be possible to maximise the energy scattered, and possibly the energy invested in the second harmonic, whilst minimising both the incident intensity and the agent concentration. Minimising the latter two features is important, since there is a general concern that the time averaged intensity to which a patient is subjected should be kept within safe levels [5], and there are certainly

restrictions on the amount of agent which can be placed within the human body. (A non-bioeffect consideration is of the cost: a few grams of agent can cost of order £100.) Since the model is nonlinear, and the definition requires knowledge of the scattered power, this can be simply calculated from the equation shown in Figure 3, which is valid for the far field. Whilst this is done for the results presented in this report, it is useful initially to consider the underlying physical processes. An intuitive understanding of these processes can be gained by considering a simple model based upon the equation of motion demonstrated in Figure 4. The radial acceleration ($\ddot{R}$) contributes to an inertial term ($m(\ddot{R})$); the wall velocity ($\dot{R}$) contributes to losses through some constant b; and there is a term dependent on the stiffness of the gas, k. The driving force is given by $P(t)$. The radius-time characteristics of the bubble motion are obtained using a nonlinear equation of motion, such as the Herring-Keller equation [6]. Each of the terms which are summed in the equation in Figure 4, has a force-like character. As such the product of b with the wall velocity gives a 'drag force' $b\dot{R}$ (actually, a pressure term). Consequently, the instantaneous power loss is given by the product of this with the wall velocity ($b\dot{R}^2$). This power loss can be integrated over time to give the energy lost from the system. If the expression for b comprises losses due to acoustic radiation, viscosity, thermal effects, and the shell (which is used to stabilise the contrast agent against dissolution), then the damping derives from b_{tot}, and the formulation will give the extinction cross-section [7]. However, if the losses under consideration are only those due to acoustic scatter, then $b = b_{rad}$, in which circumstance the acoustic scatter cross-section is derived. This is clearly a simplification, and it is more exact to use the formulation shown in Figure 4. However, the simple model of Figure 3 allows an intuitive understanding of the processes involved. Consider the top graph in Figure 3 (labelled (a)), which shows the bubble radius as a function of time. The envelope is given by the dashed line. The bubble oscillates about an equilibrium radius R_0, the amplitude of oscillation increases from the moment the insonation starts, and tends to some steady state value. The lower plot (labelled (b)) shows the square of the wall velocity, indicating a ring-up time, and the envelope of this (given by the dashed line) is proportional to the acoustics scatter cross-section σ, if the simple model in Figure 4 is used.

This simple model allows the determination of some of the key characteristics expected of bubbles in the ring-up period and beyond. Consider Figure 5. It shows three curves (blue, green, and red, indicating in rising order the use of an increasing driving amplitude). Consider the blue curve, corresponding to the use of the lowest driving amplitude. If the bubble is insonated from time zero to time t_1, then the scattered power will increase up until that time, reaching a maximum of W_1, and then fall off (as shown by the red dashed line). If however, the insonifying pulse is of duration t_2, then not only

does the duration of the scattered pulse increase; but also the maximum value achieved by the instantaneous scattered power increases (up to W_2 in the figure). This is shown by the blue dotted line in Figure 5. Therefore within the ring-up time, increasing N (the number of cycles in the insonifying pulse) increases both the duration of the scattered pulse, and the maximum amplitude it achieves. If however one were in the steady state, then the maximum amplitude achieved by the scattering would be roughly insensitive to the duration of the pulse. Increasing the duration of the insonifying pulse would, to all intents increase scattering only by increasing the duration of the scattered signal. In addition, as the driving amplitude is increased, one obtains "decreasing returns". That is to say, that the amplitude of oscillation of the bubble is limited, and doubling the energy of the incident field will not cause a doubling in the energy scattered by the bubble. This reflects the nonlinearity of the bubble process, and indeed other effects can become important (such as the fragmentation of the bubble that may occur at the highest amplitudes). These general features were tested in two experiments to be described next.

3. PRELIMINARY TESTS

Sections 3.1 and 3.2 describe two series of tests. These were undertaken to determine to what extent the broad predictions which arise from the intuitive scheme described in the preceding section are reflected in the results.

3.1 Experiments with bubbles in a population centred about 15 micrometers radius

Figure 6 shows the apparatus used in the first experiment, which involved the measurement of the response to pulses of a bubble population centred around a 15 micrometre radius. An illustration of the population distribution, measured optically, is given as an insert in Figure 6, showing the radius in micrometres against the number of bubbles on a linear scale (absolute values are not shown). The experiment took place in the A B Wood Laboratory, the source used was the 'UDI wideband shaded' sonar source, supplied by DERA, with a centre frequency of 200 kHz in this experiment. Photographs of the A B Wood Laboratory, shown empty, are given in Figure 7. Details of the experimental method can be found in a contract report associated with this work [8].

An experimental result for the scattered energy as a function of time, for insonation via pulses having a number of cycles N = 10, 20, 50, 100, 150 and 200 cycles, is shown in Figure 8. Within the ring-up period (here up to about 100 cycles), increasing the length of the incident pulse increases both the amplitude and duration of the scattered pulse. For incident pulses longer than this, increasing the duration of the incident pulse tends only to

increase the duration of the scattered pulse: the peak amplitude attained in the scatter is approximately constant. It should be noted that, because the cloud in the experiment has a finite dimension (approximately 0.5 metre radius cylindrical cloud), then this dimension will affect the rise-time and fall-time of the scattered pulses, and will tend to limit how short a scattered pulse can become as N decreases.

Figure 9 shows simulations of the scattered energy as a function of both pulse length and the peak acoustic pressure amplitude (P_{max}) of the incident field. The scattered energy is calculated simply from the pressure field scattered by the bubble, as shown in Figure 3. The model assumes that a bubble of radius 15 micrometres is insonated at 200 kHz. As expected in Figure 9a, the amplitude of the scattered energy increases for any given pulse length, with increasing amplitude of the incident field (0.5, 5 and 10 kPa are shown). As the number of cycles in the incident pulse decreases, so too does the scattered energy. This too is not unexpected. However, the scatter cross-section, shown in Figure 9b normalises the scattered power against the intensity of the incident pulse. As a result, it is a measure of the "efficiency" of the scatter, as explained earlier. Hence in consideration of Figure 9b, it is interesting to note that, as the acoustic pressure amplitude increases in the range studied, the steady state efficiency decreases. Another interesting effect can be seen most clearly in the plot of scattered energy (Figure 9a) at the highest amplitude (10 kPa, the blue line). At pulse cycles below $N = 20$, the scattered energy is increased above that which would be expected if the trend which is seen for longer pulses, is extrapolated back to the origin (as shown by the dotted blue line). When the efficiency is plotted (in Figure 9b), this results in a peak in the scatter cross-section at around 10 cycles. The peak in efficiency occurs at a shorter pulse length as the amplitude of the incident field increases. Hence there is a maximum in the efficiency, which becomes more pronounced as the sound field amplitude is increased.

In contrast the energy invested in the second harmonic (Figure 10a), and the corresponding scatter cross-section (based on the energy scattered at twice the incident frequency, Figure 10b) both simply increase with increasing amplitude of the incident field, and the increasing number of cycles. Though a slight effect is seen in this cross-section (Figure 10b) around 15 cycles, this is very much less than the maximum seen in Figure 9b for the scattering of the total energy in the pulse.

Figure 11 summarises the conclusions that can be made from experiment 1 (scattering of energy from bubbles of 15 micrometre radius). Within the parameter range studied, the efficiency of the scatter within the ring-up period is increased by using longer pulses, and lower amplitudes. Steady state efficiency increases as the amplitude of the incident field is decreased. As the length of the incident pulse increases beyond the ring-up period, the

efficiency reaches an approximately constant value, which decreases with increasing amplitude of the incident field. Hence for the same temporal average intensity of the incident field (I_{TA}), the maximum in the curves in Figure 9b suggests the following. It is possible to obtain enhanced scatter if one uses pulses of lower amplitudes but greater pulse repetition frequency, provided that the duration of the incident pulse is set to the value which gives the maximum in Figure 9b (or equivalent).

Enhanced scatter would be an exciting prospect for the use of contrast agents, where one has to keep the 'doses' of ultrasound and of contrast agent to a minimum (within the constraints of retaining a clinically useful signal). Whilst such optimal values appear not to exist for the second harmonic (Figure 10) the results of the first experiment suggest that the following hypothesis might be made (Figure 12). This is to say that there exists a certain input pulse, defined by its duration and amplitude, which will maximise the ratio of the total energy scattered in the pulse, to the energy in the incident pulse. This might allow one to maximise the signal-to-noise ratio (SNR) in the ultrasonic signal returned from the bubbles, whilst minimising the amplitude of the driving field and the bubble concentration. It would also cause the contrast agent to scatter with maximum enhancement over the scatter obtained from tissue.

The experimental work suggests that this works for bubbles having radii distributed around 15 micrometres, and our knowledge of bubble dynamics suggests it should also work for larger bubbles. Two questions however remain. First, does such an effect occur for the contrast agents currently used in clinical applications? Second, does it occur with a useful temporal peak intensity of the incident field (I_{TP})? The latter point is important. Whilst the results of Figure 9b suggest that reducing the amplitude of the incident field enhances the efficiency, the results of Figure 9a show that the *absolute* value of the scattered energy decreases as the amplitude of the incident field is decreased. Hence with very low amplitude fields, we might be obtaining very efficient scattering, but the signal-to-noise ratio in the received data might be so low as to give no useful information to the clinician. Whether this hypothesis has any validity is discussed in the following section.

3.2 Experiments using contrast agents

Samples of the contrast agent Levovist ™ (Schering) were obtained and used in a 10 gram per litre concentration. The Levovist was held within dialysis tubing, which provided a containment wall with negligible acoustic effect. A range of acoustic sources were used in the frequency range 2 to 3 MHz in continuous wave stepped tone, and pulsed, mode. Experiments were undertaken by Miss S Ponthus for her MSc project, under the supervision of Dr Leighton. The apparatus is shown in Figure 13. The results

of this experiment can be found in Ponthus' project report [9]. She obtained resonance curves for side scatter and attenuation, from which the damping and resonance frequency of the contrast agents could be determined. These were then used as input parameters within the model for the nonlinear scatter cross-section [7], to provide the results presented below.

The contrast agent population contained a majority of bubbles of radius approximately 0.8 micrometres. The model therefore uses such bubbles, insonated at resonance (2.3 MHz) to demonstrate whether there is any enhancement effect. Figure 14 shows the total scattered energy (14a), and the scatter cross-section relevant to the entire pulse (14b), as a function of the amplitude of the incident field and the number of cycles in the incident pulse. The results are quite different from those seen with larger bubbles in Figure 9. As expected in Figure 14a, the amplitude of the scattered energy increases with the amplitude of the sound field and with the number of cycles. However, the results for the efficiency (Figure 14b) are quite different. First, the steady state value of the scatter cross-section increases with increasing incident sound field amplitude (the reverse of what was seen in Figure 9b). It should be noted that the acoustic pressure amplitude range used here for contrast agents (10 to 60 Pa) is higher than that used for the larger bubbles in experiment 1 (0.5 to 10 kPa). This reflects the practical limits of the conditions that can be generated for the respective bubbles, and clearly if this study were to be extended, a fuller investigation of the effect of the amplitude of the incident field would be required. The second difference is between Figures 14 and 9, is as follows: for the contrast agents, the steady state value of the cross-sections is achieved for pulses greater than only about 4 or 5 cycles in length; and that for shorter pulses, the scattered cross-section simply increases with decreasing pulse length. This is quite different to the effects seen for larger bubbles where, as N decreases the efficiency rises from the steady state to a maximum value at around 10 to 15 cycles; and reduces for smaller pulses. The immediate implication of this is that the conditions under which contrast agents are normally insonated (high amplitude, short pulses) might fortuitously give the conditions that maximise the efficiency in the scatter. However, as stated above, the model would have to be extended to higher amplitudes to confirm this.

The energy in the second harmonic (Figure 15a), and the cross-section relevant to the second harmonic (Figure 15b) both increase as the duration and amplitude of the incident pulse is increased. This trend is the same as was seen for larger bubbles (Figure 10).

Figure 16 summarises the difference seen between bubbles of radius 15 micrometre insonated at resonance, and bubbles of 0.8 micrometre radius insonated at resonance. To follow-up on the point made earlier, that the study should be extended to higher

amplitudes, the plot of the acoustic cross-section for 15 micrometre bubbles relevant to an incident acoustic field of amplitude 60 kPa is also shown (green line in 16a): clearly the trend for producing a maximum has been suppressed. Also shown on each plot is the value of the acoustic scatter cross-section, as predicted by linear theory (purple arrow). In both cases, it is less than that predicted by the nonlinear theory. This again raises a curious difference between the larger and the smaller bubbles. For the smaller bubbles, as the amplitude of the sound field is increased, the steady state value of the scatter cross-section deviates increasingly from that predicted by the linear theory (16b). However, the converse is true for the larger bubbles (16a).

Figure 17 throws some light on the difference between these bubbles. The figure shows, as a function of the amplitude of the driving field, the amplitude of the scattered energy (red line) and the scattering cross-section (black line), both as pertain to the values reached in the steady state. This is done for bubbles of 15 micrometres, 3 micrometres, and 0.8 micrometres radius, insonated at resonance. In all three cases, as expected, the total energy scattered by the bubble increases with the amplitude of the driving field. However, the cross-section decreases with increasing pressure amplitude for the 15 micrometre bubble, whilst the reverse is true for the 0.8 micrometre bubble. These two trends cancel out bubbles of radius 3 micrometres, where the acoustic scatter cross-section is independent of the driving field amplitude.

3.3 CONCLUSIONS

The conclusions are summarised in Figure 18. Those relating to the second harmonic are relatively simple. Both the amplitude and efficiency of scatter increase with increasing amplitude and duration of the incident pulse (Figure 18a). Within the parameter range studied, certain conclusions might be drawn for the efficiency and scatter of the energy within the pulse (i.e. the "frequency-insensitive" scatter and cross-section). However, these must be treated with caution, as this study represents simply a brief test of whether the formulation for the nonlinear acoustic cross-section reveals any trends in specific test cases which might suggest areas of future research. Both the range of bubble sizes and the amplitude of the incident fields are limited in this study, and are insufficient to cover the entire range of parameters that might be observed in particular applications. With this in mind, the following trends have been seen (Figure 18b). For times greater than the ring-up time, the acoustic scatter cross-section (or efficiency) tends to a steady state value. For bubbles greater than 3 micrometres in radius, this value decreases with increasing amplitude of the driving field. For bubbles smaller than 3 micrometre radius, the steady state value of the efficiency increases with increasing amplitude of the driving field.

For shorter pulses the behaviour is complicated. For the two cases studied here, insonation of the larger bubble the efficiency showed a maximum as a function of the number of cycles of the incident pulse; and for the smaller bubbles, the efficiency increased with decreasing length of the incident pulse. However, as shown in Figure 16a, even these simple trends can fall down at the higher amplitudes of the driving fields. In addition, any attempt to maximise or minimise the efficiency must bear in mind the absolute value of the scattered energy: a high efficiency but low absolute scatter may not deliver a useful signal to the detector. However, within the parameter space studied here, it is possible to postulate general schemes for maximising efficiency (Figure 18c). There exists some critical bubble radius, which in this study appears to occur at around 3 micrometres. For bubbles larger than this, efficiency is maximised by using low amplitude pulses. For bubbles smaller than this efficiency is maximised by using short high amplitude pulses. This has implications for the use of contrast agents, which in general are subjected to short, high amplitude pulses. However, as new modalities and technologies develop, the pulse regime to which contrast agents might be subjected is likely to vary considerably.

The final conclusions would be that the linear models appear to give poor predictions of the scatter and the efficiency; and that the study needs extending to higher amplitudes.

REFERENCES

[1] Parker, K.J., Baggs, R.B., Lerner, R.M., Tuthill, T.A., Violante, M.R. Ultrasound contrast for hepatic tumours using IDE particles. *Investigative Radiology* 1990, **25**, 1135-1139

[2] Ophir, J., Parker, K.J. Contrast agents in diagnostic ultrasound. *Ultrasound in Med. & Biol.* 1989, **15**(4), 319-333.

[3] Gramiak, R., Shah, P.M. Echocardiography of the aortic root. *Investigative Radiology* 1968, **3**, 356-366.

[4] de Jong, N. Acoustic properties of ultrasound contrast agents. (Zuidam & Zonen bv, Woerden) 1993.

[5] Wells, P.N.T. The prudent use of diagnostic ultrasound. *Ultrasound in Med. & Biol.* 1987, **13**(7), 391-400.

[6] Leighton, T.G. *The Acoustic Bubble* (Academic Press, London). 1994. Chapter 4.

[7] Clarke, J.W.L. and Leighton, T.G. The Enhancement of Sonar Detection in Bubbly Environments Part 2: Effect of Salinity on Damping and Development of Models. *ISVR Contract Report No. 98/31, University of Southampton*, 1998.

[8] Clarke, J.W.L. and Leighton, T.G. The Enhancement of Sonar Detection in Bubbly Environments Part 3: Experimental measurements of acoustic backscatter from bubble clouds. *ISVR Contract Report, University of Southampton* (in press), 1999.

[9] Ponthus, S.. Characterisation of the acoustic properties of ultrasonic contrast agents. *MSc Project Thesis, University of Southampton*, 1998.

Figure 1: Two options for cross-section:
Both based on scattered power

	Nonlinear	Underlying bubble physics
$\frac{Power(n^{th}\,harmonic)}{Power(fundamental)}$	√	×
$\frac{Scattered \cdot power}{Incident \cdot plane \cdot wave \cdot int ensity}$	×	√

Figure 2: Basic definition

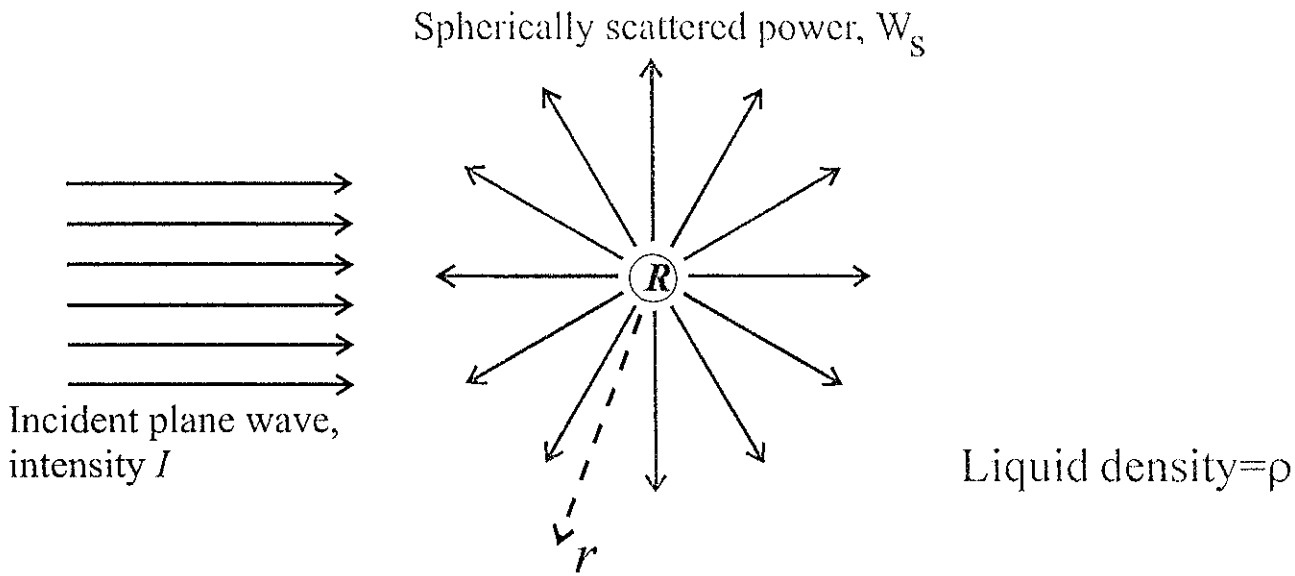

Scattering cross-section: $\sigma = W_s / I$

Dimensions: $\frac{\text{Power}}{\text{Intensity}} \rightarrow$ Area

Can be extended to bubble cloud (multiple scatter corrections?)

Figure 3: Proposed modifications (Nonlinear acoustic scatter cross-section)

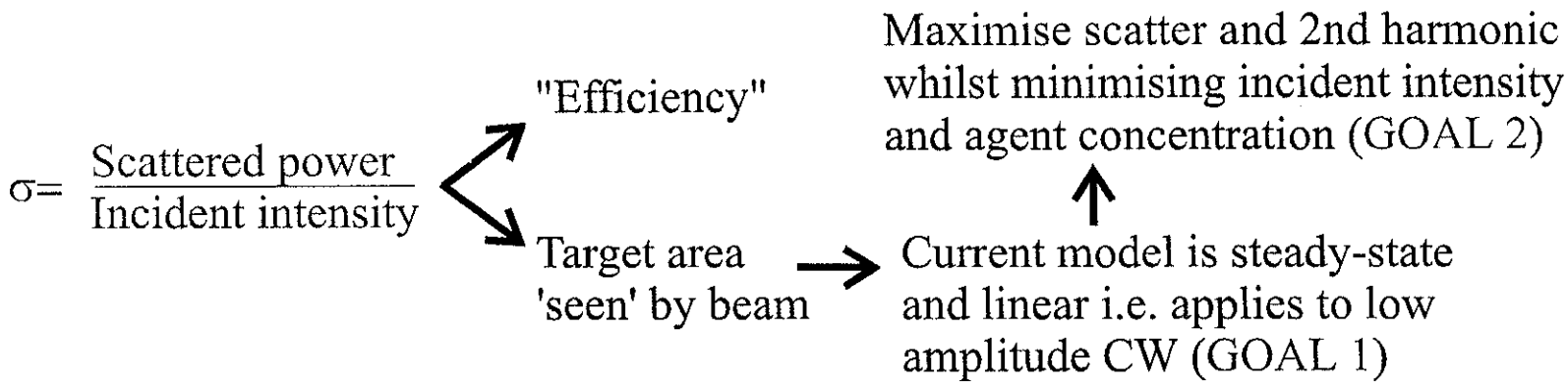

Requires calculation of Scattered power:

Full nonlinear calculation:

Use: Pressure scattered by bubble = $\rho \frac{R}{r}\left(\ddot{R}R + 2\dot{R}^2\right)$

(valid for r>>R)

Figure 4: Require scattered power:
Simple model

Obtain R from nonlinear equation

$$m\ddot{R} + b\dot{R} + kR = P(t)$$

Driver

Drag 'force': $b\dot{R}$

Instantaneous power loss: $b\dot{R}^2$

Integrate

Extinction cross section:

Use $b = b_{tot} = b_{rad} + b_{vis} + b_{th} + b_{sh}$

Scatter cross section: $b = b_{rad}$

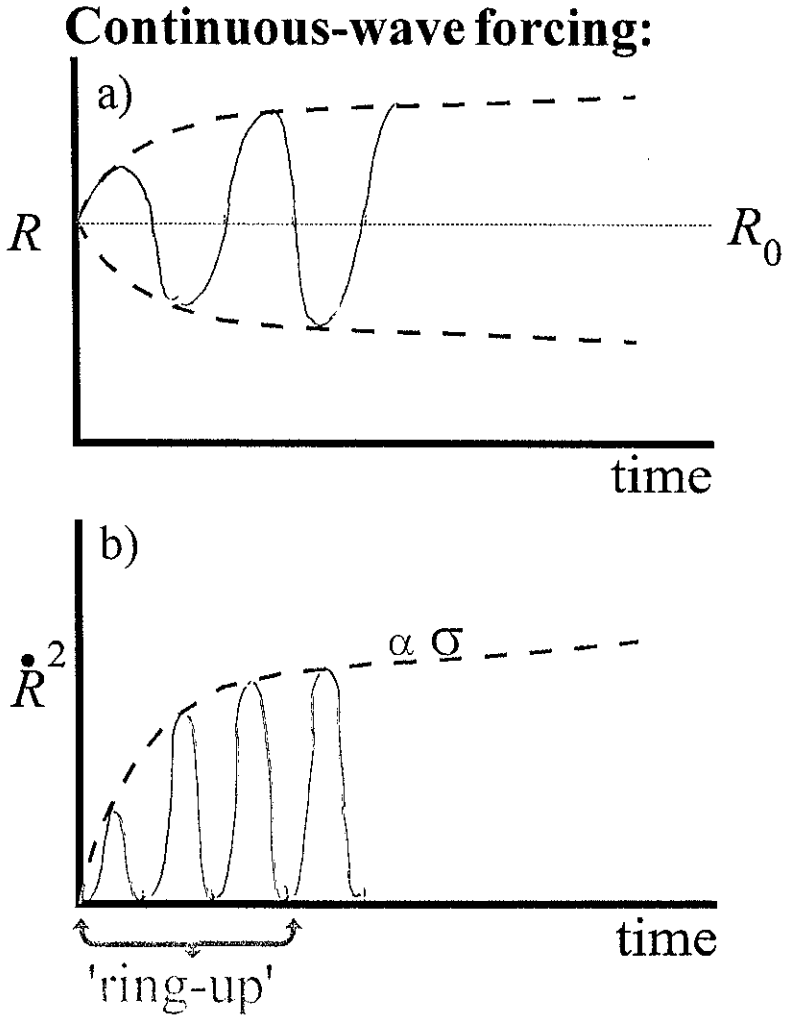

Figure 5: Bubbles differ from linear systems at high amplitude

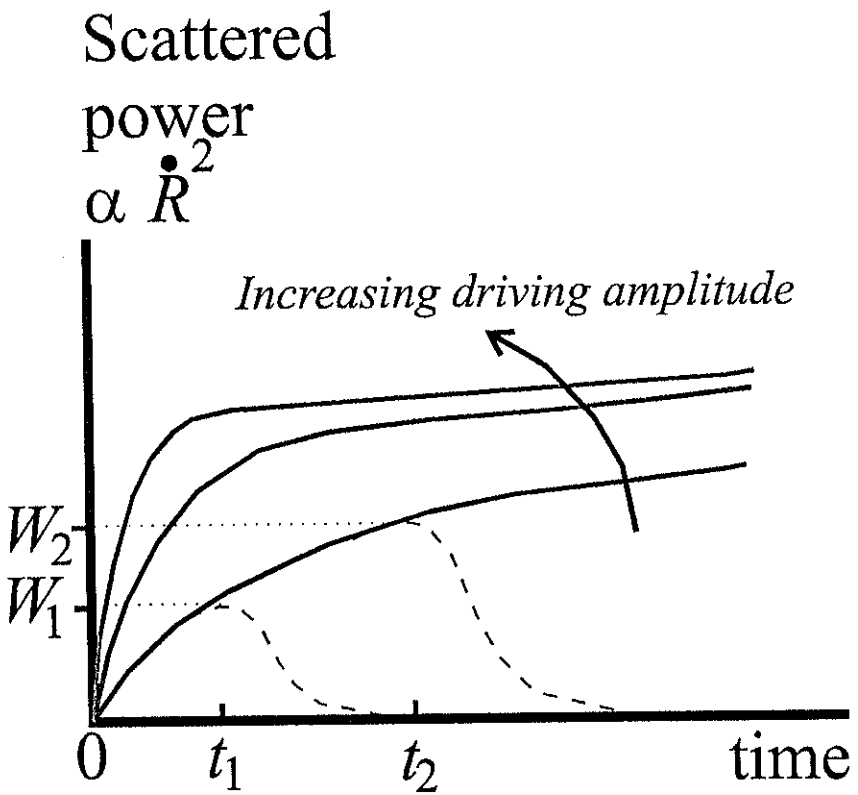

- Within ring-up time, increasing N increases scatter efficiency
- Increasing the driving amplitude:
  - reduces this effect
  - gives decreasing returns
- 2 Experiments

Figure 6: Experiment 1- Apparatus

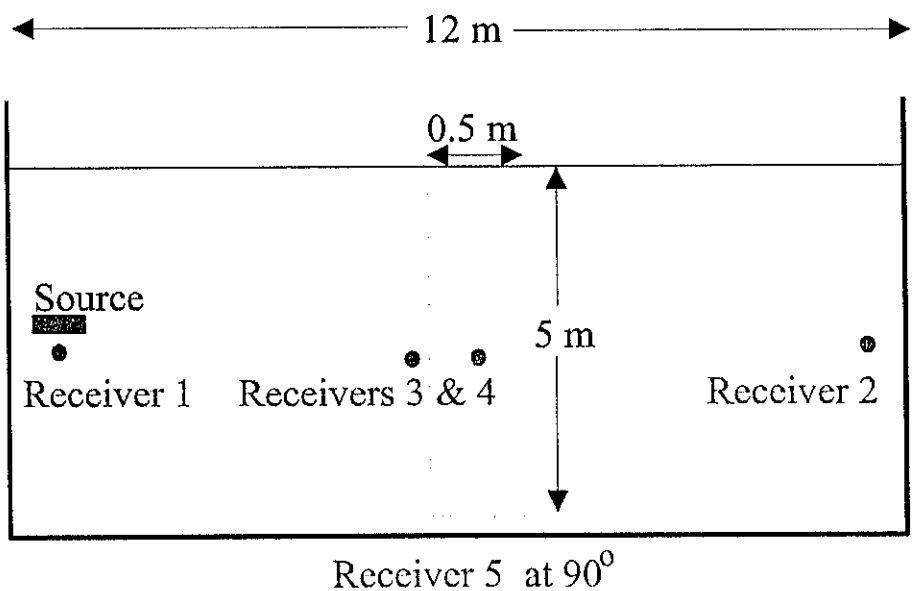

- Source:

Q=1; 200 kHz
(centre frequency)

- Tank:

8x8x5 m^3

- Bubbles:

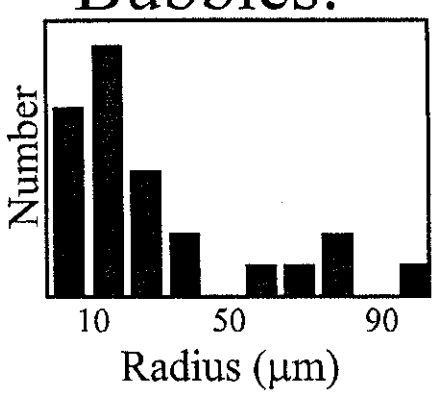

Figure 7: Experiment 1- Photographs of tank

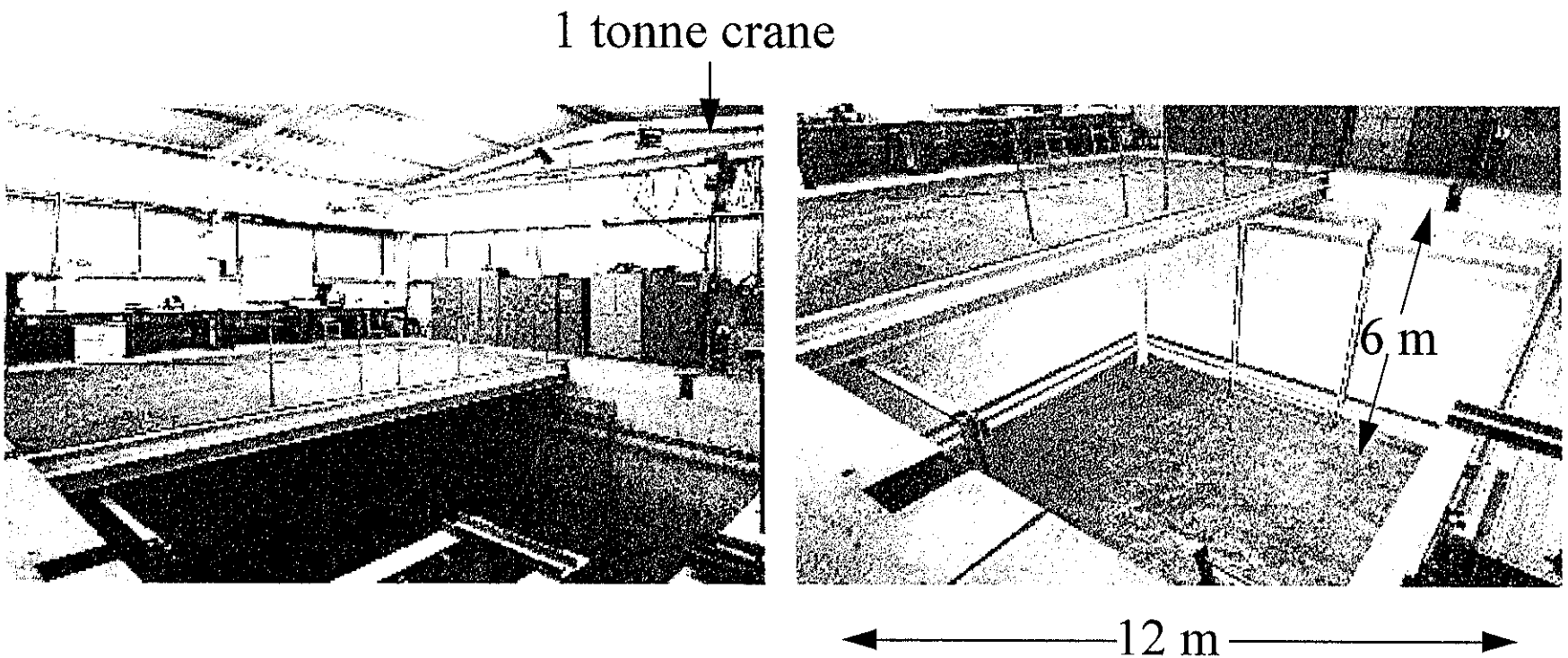

Figure 8: Results - Constant driving amplitude, varying *N*

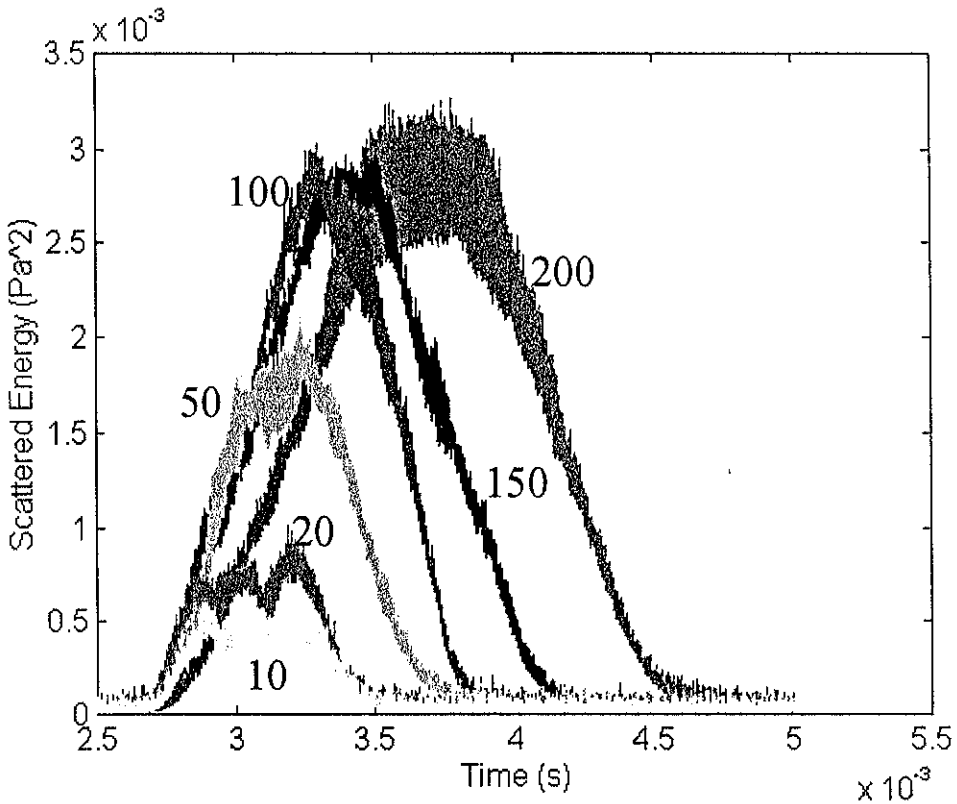

Effect of increasing N:

Within ring-up period:

- Increases scatter amplitude and duration

Beyond ring-up period:

- Increases duration only

(cloud dimension affects duration)

Figure 9

Frequency-insensitive case (all energy in pulse):
Vary both P_{max} and N (15 μm, 200 kHz)

(a)

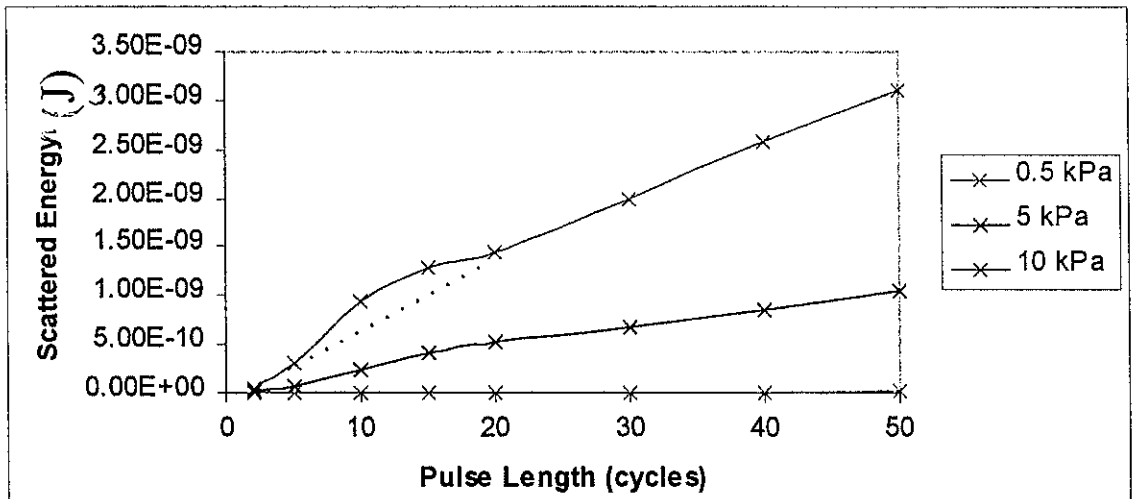

Scattered energy

(b)

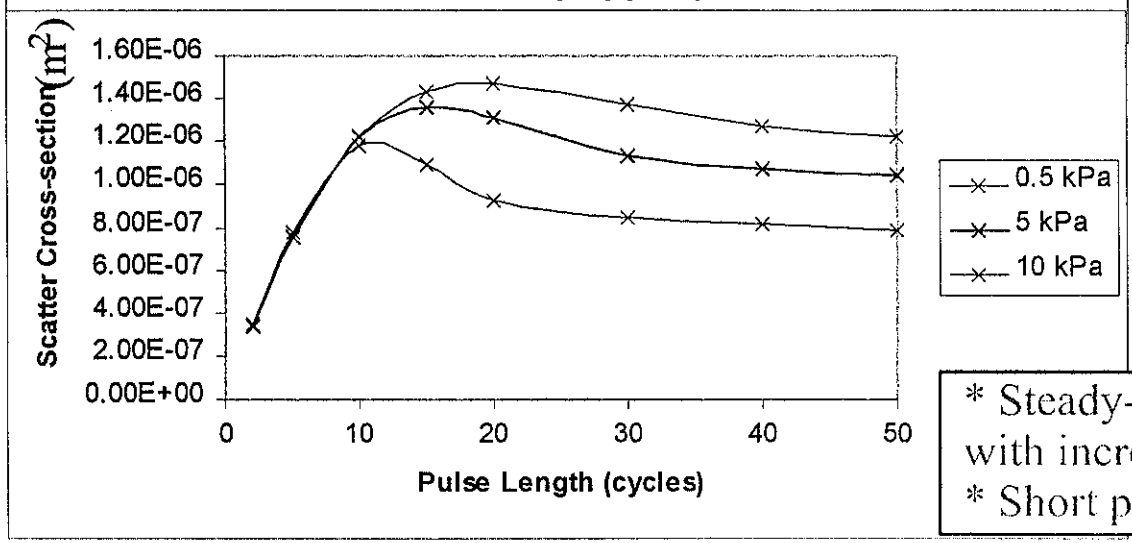

'Efficiency' = scatter cross-section

* Steady-state value decreases with increasing driving amplitude
* Short pulses enhance efficiency

Figure 10

SECOND HARMONIC: Vary both P_{max} and N (15 μm, 200 kHz)

(a)

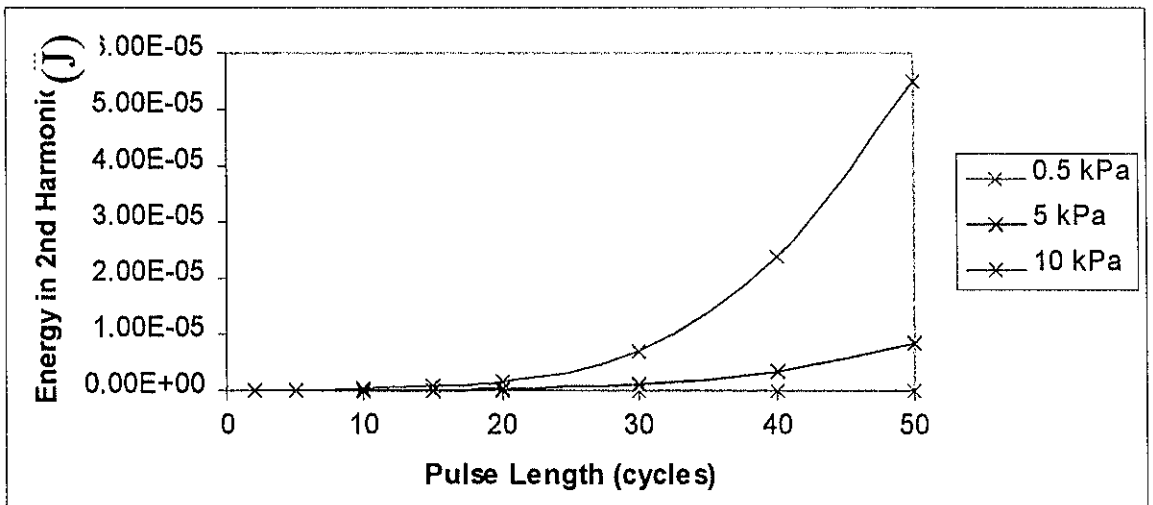

Scattered energy

(b)

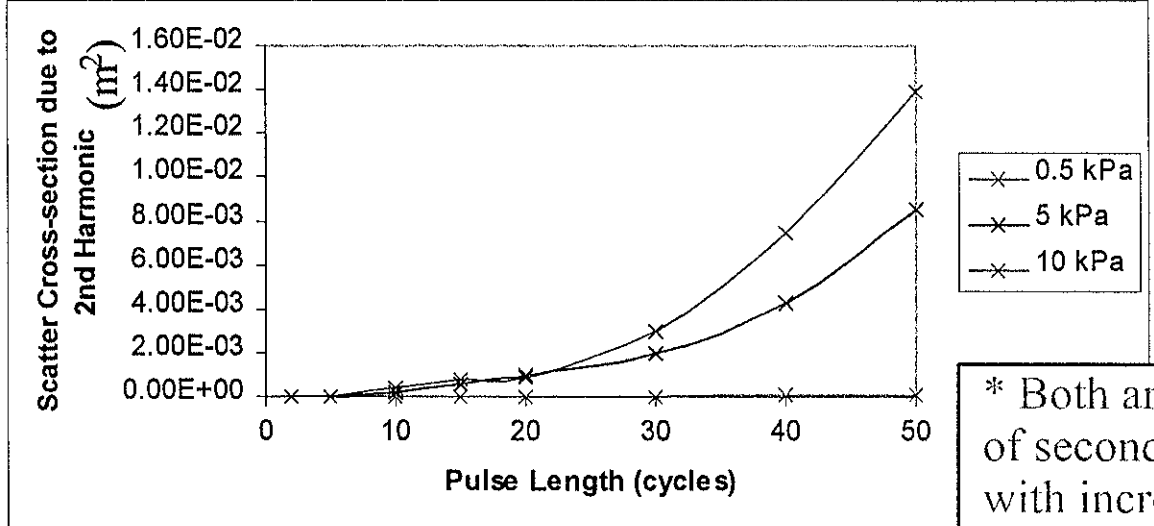

Efficiency

* Both amplitude and efficiency of second harmonic increase with increasing driving amplitude

Figure 11

Conclusion from experiment 1

- Efficiency of scatter is increased by using:
  - longer pulses (within ring-up time),
  - lower amplitudes.
- Obtain enhanced scatter for same I_{TA}

(SNR, Resolution, cloud ringing)

Figure 12

Proposal

There exists an optimal input pulse length and amplitude to maximise the ratios:

$$\frac{\text{ENERGY SCATTERED IN PULSE}}{\text{ENERGY INPUT}}$$

i.e. One could maximise SNR whilst minimising amplitude of driving field & bubble concentration

Work for R_0>15μ*m..... But for contrast agents? at useful* I_{TP} *?*

Figure 13

Experiment 2: Levovist (10 g/l)

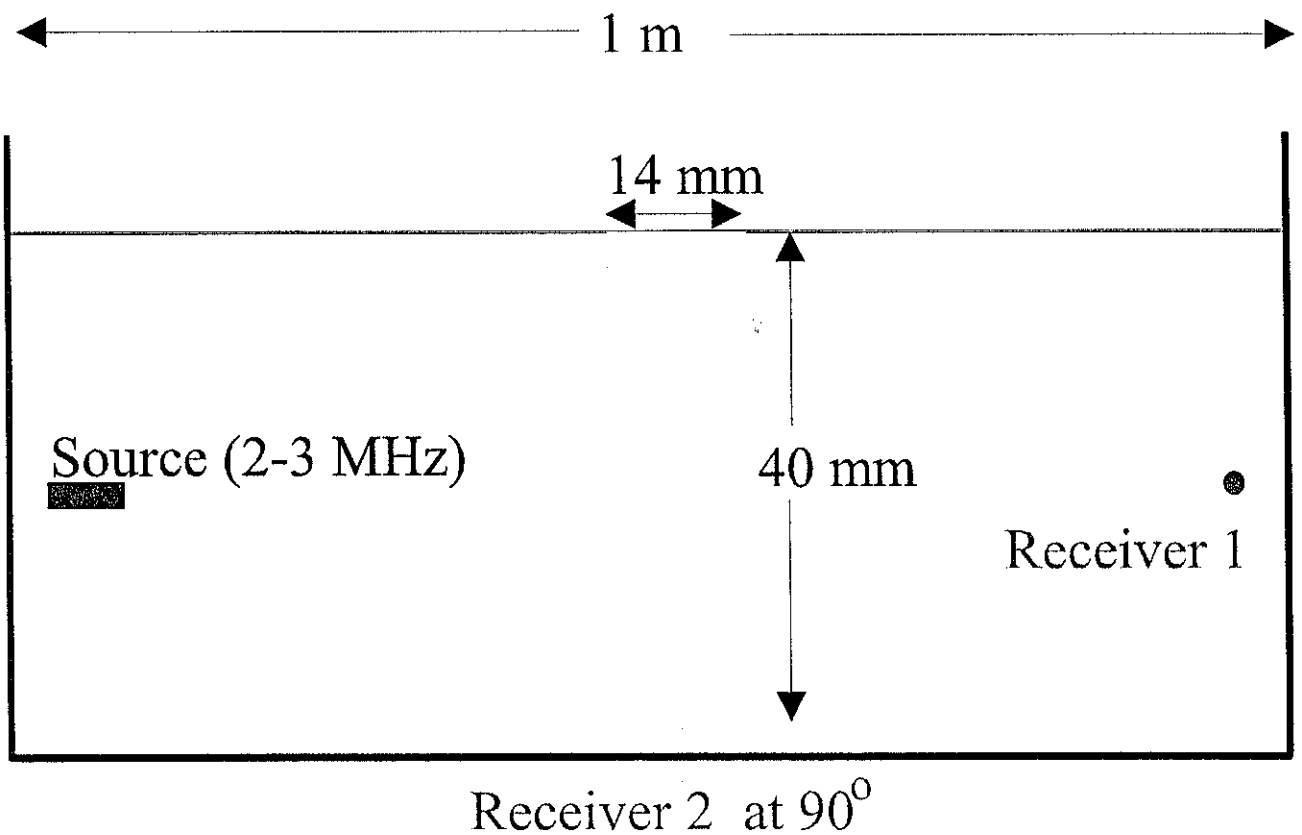

Figure 14

Total and proportional energy scattered (0.8 μm, 2.3 MHz)

(a)

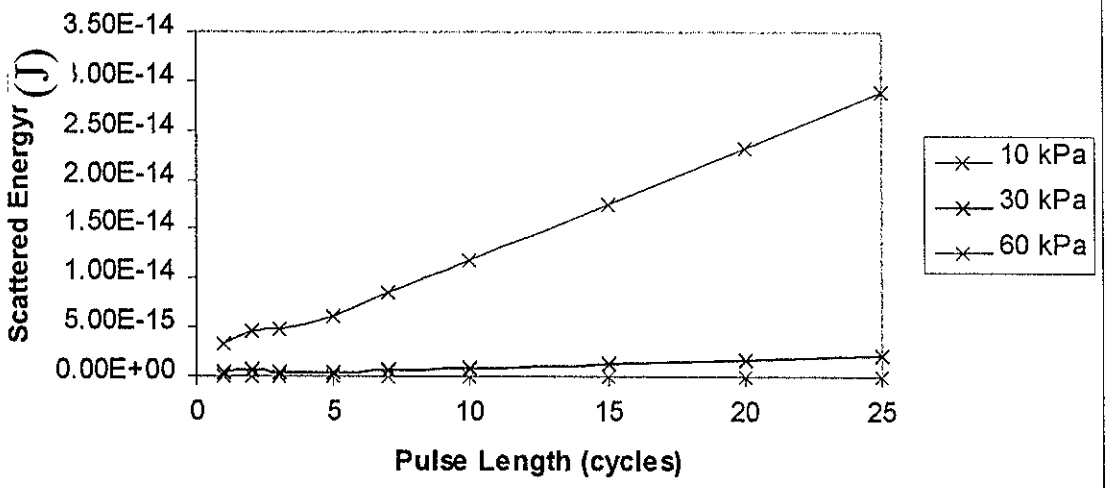

Scattered energy

(b)

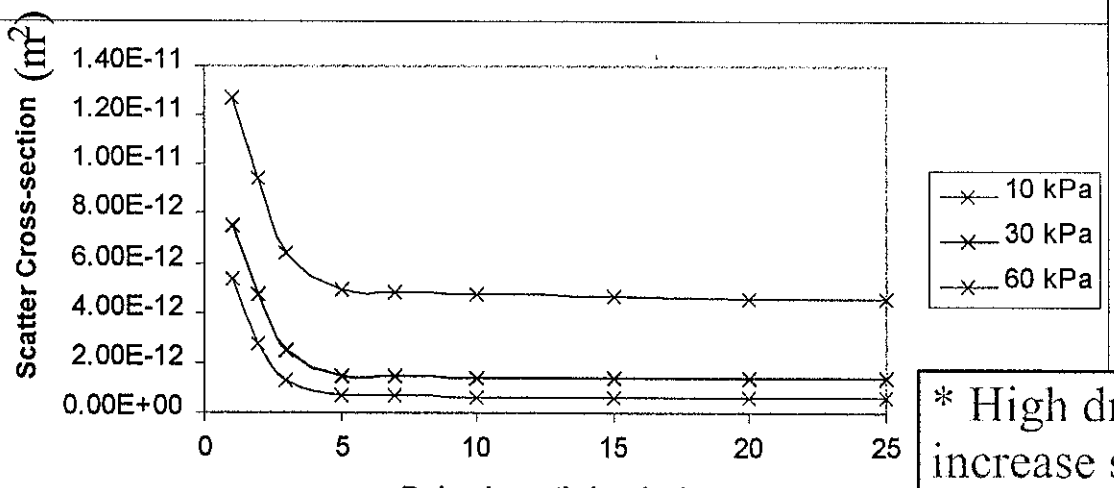

Efficiency

* High driving amplitudes increase scatter
* Short pulses enhance efficiency

Figure 15

Second harmonic (0.8 μm, 2.3 MHz)

(a)

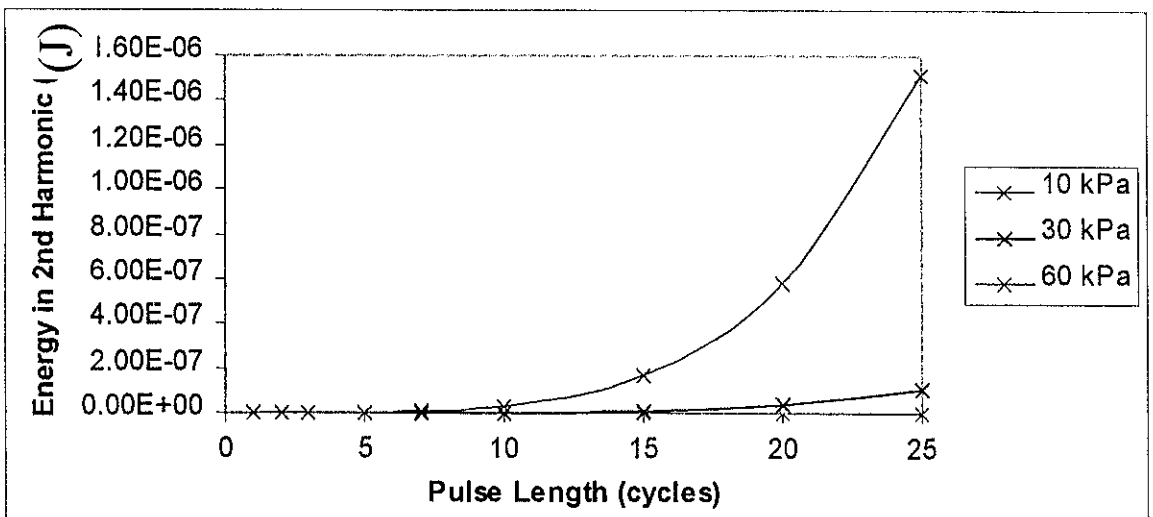

Scattered energy

(b)

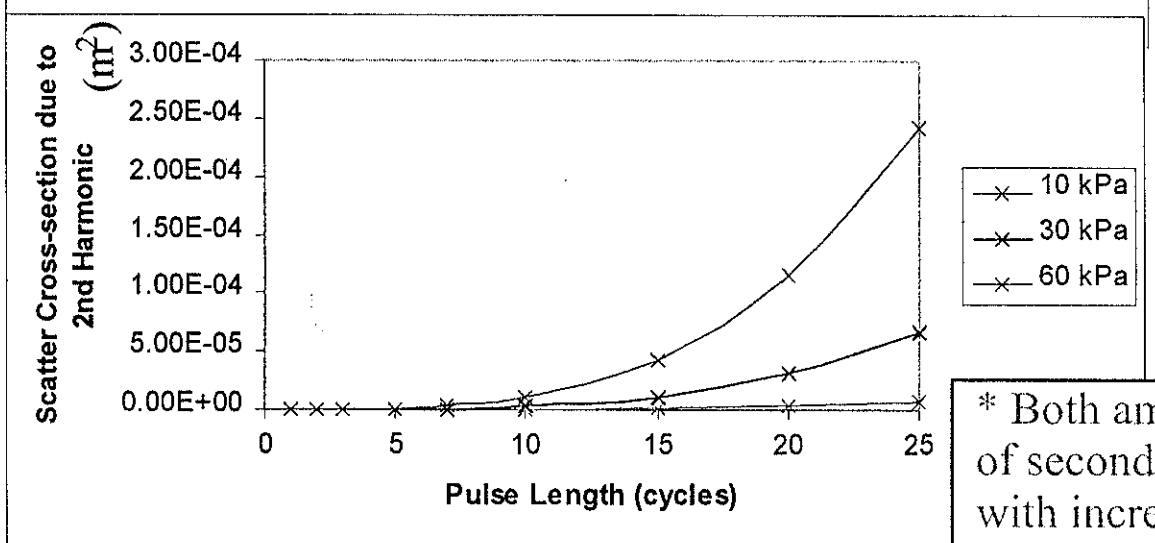

Efficiency

* Both amplitude and efficiency of second harmonic increase with increasing driving amplitude

Figure 16

Radius dependent effect:
Scattering cross-section (all energy)

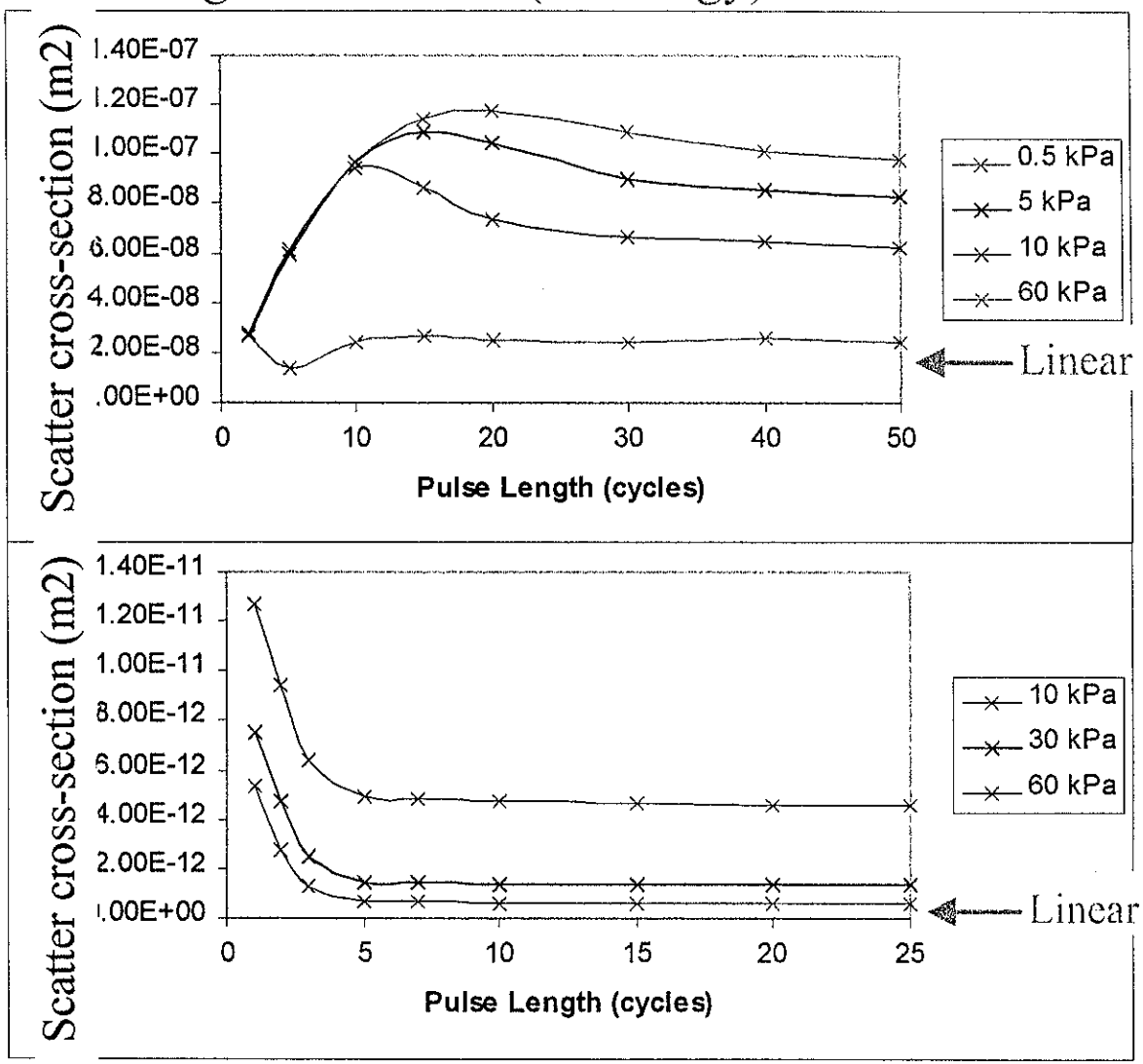

Figure 17

Radius dependent effect:
Steady state radiated pressure and scattering cross-section

(a)

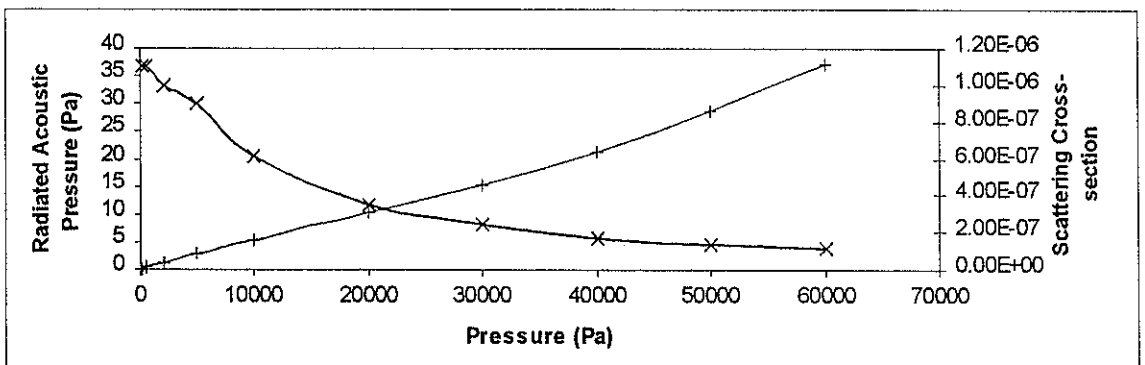

15 μm,
200 kHz

(b)

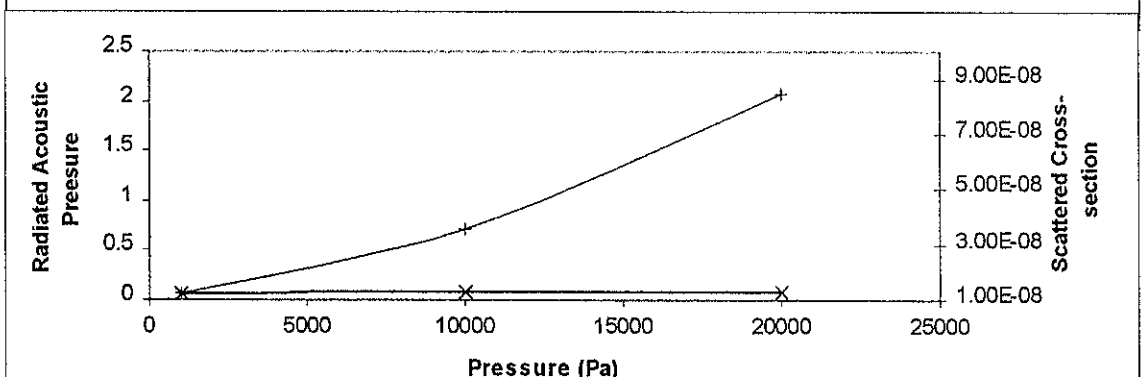

3 μm,
850 kHz

(c)

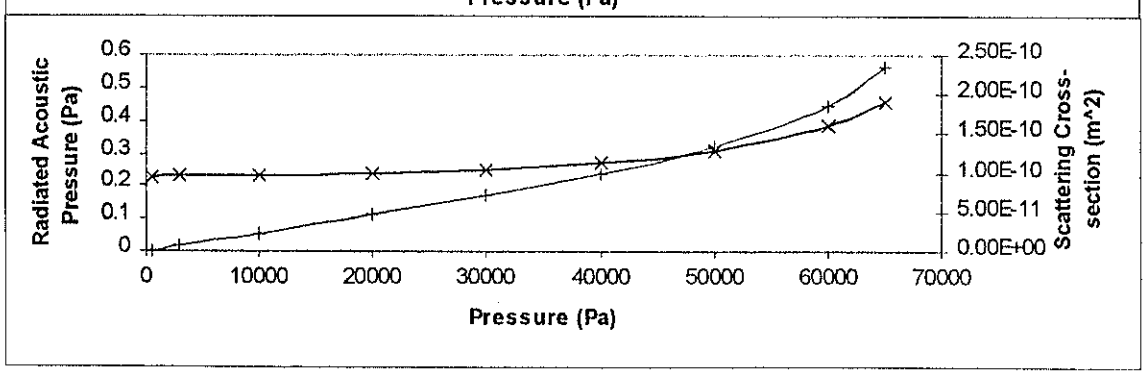

0.8 μm,
2.3 MHz

Figure 18a

Conclusions (<70 kPa driving amplitude):
2nd harmonic

- Amplitude and efficiency of scatter increase with increasing incident pulse length and amplitude

Figure 18b

Conclusions (<70 kPa driving amplitude): Efficiency and scatter (frequency-insensitive)

- For large N (>10), efficiency of scatter (all energy) tends to a steady state value.

  R>3 μm This value decreases with increasing driving amplitude

  R<3 μm This value increases with increasing driving amplitude

- For shorter pulses the behaviour is complicated, and scatter efficiency may be maximised or minimised by choice of pulse length and amplitude. CAUTION: Reducing either reduces SNR, though increasing prf may compensate.

Figure 18c

For maximum efficiency....

For R>3 μm efficiency is maximised by using long, low amplitude pulses...

... for R<3 μm, use short, high amplitude pulses for maximum efficiency

Linear models give poor predictions

Study needs extending to higher amplitudes.